Journal of Basic and Environmental Sciences, 5 (2018) 134-148

ISSN
Online: 2356-6388
Print: 2536-9202

Research Article Open Access

Characterization of The Interaction Between Surface Water and Groundwater Using Major Ion Chemistry and Stable Isotopes Northwest Sinai Egypt

H.A.Ezzeldin[a], M.A.Gomaaa [a], E.Zaghlool[a], R.El-Sheikh[b] and A.S.Amine[c]

[a] Desert research center, Egypt.
[b] Faculty of science Zagazig University, Egypt.
[c] Faculty of science Benha University, Egypt.
Corresponding author: h.ezzeldin@hotmail.com

Abstract

The relationship between groundwater and surface water in the area north west of Sinai were studied based on major ion chemistry and stable isotopes. The physico-chemical characteristics of the groundwater in the study area indicate that different hydrochemical conditions exist defining geochemical zones with distinct groundwater types. Groundwater samples in the area were classified according to its origin as 78% meteoric and 22% marine, the majority of groundwater samples belong to the more advanced grade of meta-somatic sequence ($Cl^- > SO_4^{--} > HCO_3^-$). The least mineralized water is found close to El-Salam canal, which is considered as the main recharging source, and the salinity of groundwater increases significantly with distance away from the canal.

Geochemical reaction models have been constructed using major anions and cations and stable isotopes data concentrations observed in the groundwater and surface water samples. These data were processed along flow path to assess the hydrogeochemical processes and calculate the mixing ratios with the different surface water sources. Halite, Calcite, Montmorillonite, Cation exchange, Gypsum, Biotite, Dolomite and Alunite minerals were included as phases in NETPATH model due to the aeolian deposits (sand dune and sand sheets) and alluvial plain deposits (sand mixed with silt and dark clay) that cover most parts of the study area. Mixing phenomena reflected the impact of El-Salam canal as well as sea water on the groundwater quality in the study area.

Keywords: Groundwater, Surface water, Interaction, Major ion chemistry, Stable isotopes, Modeling, Norwest Sinai
Received; 19 December. 2017, Revised form; 28 Mar. 2018, Accepted; 28 Mar. 2018, Available online 1 Apr. 2018

1-Introduction:

Growing population and large development agriculture programs are now being undertaken occurring in the North-West Sinai especially after El-Salam canal irrigation project which is considered as one of the five-mega irrigation projects in Egypt. This project is initiated in 1987 in order to carry the irrigation water to Sinai Peninsula for realization horizontal agricultural expansion by mixing the Nile fresh water from the Damietta branch with the drainage water from Bahr Hadous and El Serw drainage water with a ratio of about 1:1 nearly [1].

To utilize and protect valuable water resources effectively and predict the change in groundwater environments, it is necessary to understand the hydrochemical characteristics of the groundwater and its evolution under natural water circulation processes.

The ultimate objectives of this study were to characterize the hydrogeochemical evolution of groundwater, identify factors affecting the quality of the aquifer and study the effect of growing population and increasing agricultural activities on deterioration of water resources in the study area. Stable isotopes including oxygen-18 and deuterium were used as a supplementary tool along with conventional chemical approach to understand the origin of water, recharging sources, mixing ratios or processes that have affected water since it was percolated into the groundwater aquifer.

Study area:

The studied area lies in northwestern portion of Sinai Peninsula between latitudes 30° 40′ to 31° 05′ N longitudes 32° 20′ to 33° 00′ E bordered from the north by the Mediterranean Sea, from the south by Ismailia, from the west by the Suez Canal and from the east by Bir El-Abd with an approximate area of (1500 km^2) (Figure 1).

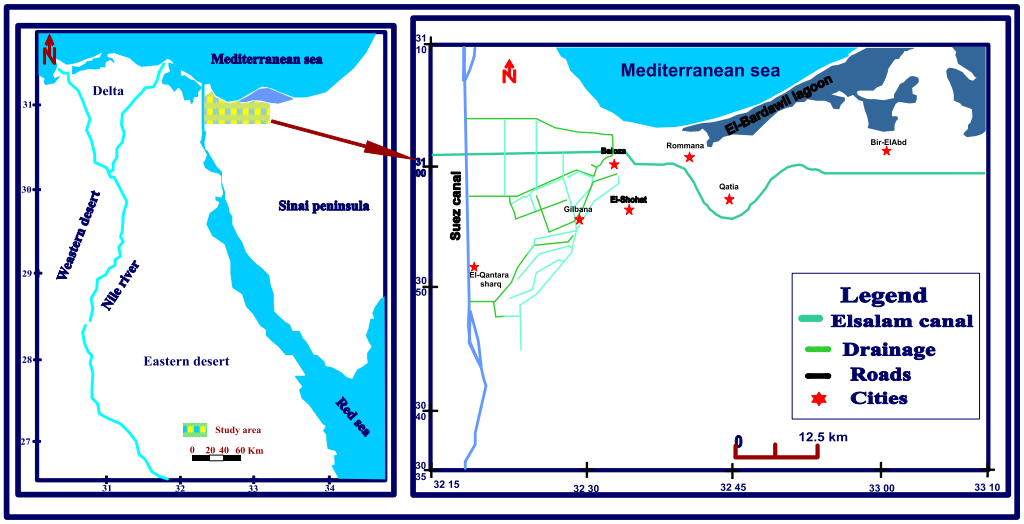

Fig (1): Location map of the study area.

II- Geomorphological, geological setting:

Geomorphologically, the study area is characterized by low relief, in which the surface elevation varies from (+1m) to (+30m), development of salt marches and sabkhas as well as by sand sheets and sand accumulation [2].

Geologically, the north-western portion of Sinai Peninsula considered as a huge sedimentary basin in which the sedimentary column reaches about 3000m and the oldest rocks are the Jurassic near the southern border [3]. The study area shows different geological units of different ages, the Holocene **facies** (Sabkha deposits sand dunes and sand sheets), Pleistocene deposits (sand and grits with minor clay interbeds and Sahl Al-Tinah formation, which is composed of mixture of black and white sands and silts) and **Pliocene deposits** (shale intercalated with marl and fossiliferous limestone) [4], (Figure 3).

2- Hydrogeological aspects:

The Quaternary deposits (sand, gravel and calcareous sandstone) and the Holocene-recent sand dunes are the main aquifers extending along the Mediterranean from Bir El-Abd to El-Qantara [3].

There are two main Quaternary aquifers in the north-western portion of Sinai

The northwestern portion of Sinai embodies many distinctive geomorphological units, sand dune sabkha deposits, coastal sand dune deposits, wadi deposits, pluvial deposits, desert lake deposits and EL- Tina Bay [3], (Figure 2).

a- Shallow sand aquifer (dune aquifer):

The thickness of this aquifer ranges from 1.4 m in the northwest to reach about 60m in the extreme southeast. The direction of water flow in this aquifer is mainly toward the northwest direction and the fresh water was found as a thin layer floating over the saline water due to the direct rainfall during rainy seasons. [5].

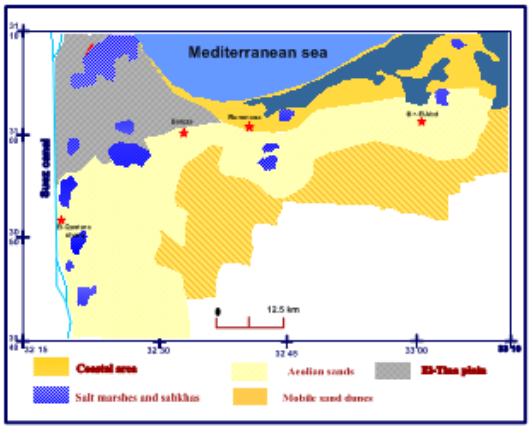

Fig (2): Geomorphological map of the study Area modified after [6].

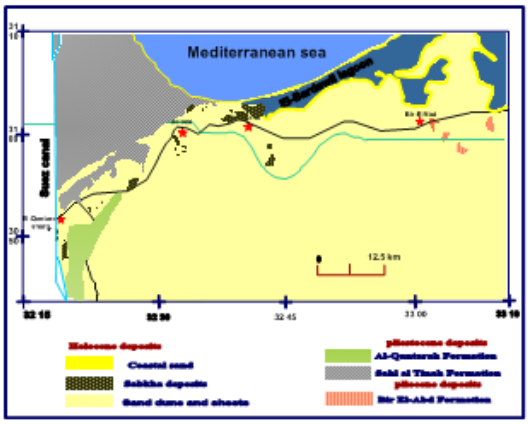

Fig (3): geology map modified after [4].

b- Deep aquifer:

Coarse sand and gravels layer saturated with fresh water represents the Pleistocene deep sand aquifer in the study area. The fresh water of this Pleistocene aquifer is expected to be originating from the Pliocene aquifer that is

connected with the Pleistocene shallow aquifer through fractures that characterize this area. The depth to the surface of this aquifer ranges from 11.6 to about 165m with an average depth of about 91m. [5].

From field measurements for the study area the groundwater level descends from 12.97 m (well no. 42) to -1.88 m in the west (well no. 11). The general direction of groundwater movement is from the southeast to the northwest, from the new reclaimed areas around south El-Qantara canal to the Suez Canal passing through the new El-Qantara city without specific direction in the middle of the investigated area. The flow pattern facilitates the formation of water-logged areas, the flow directions indicate that the area south El-Qantara Canal and the newly cultivated lands act as a recharge front for groundwater aquifer, while the northern parts, including Baloza drain and Suez Canal form the discharge areas [7], (Figure 4).

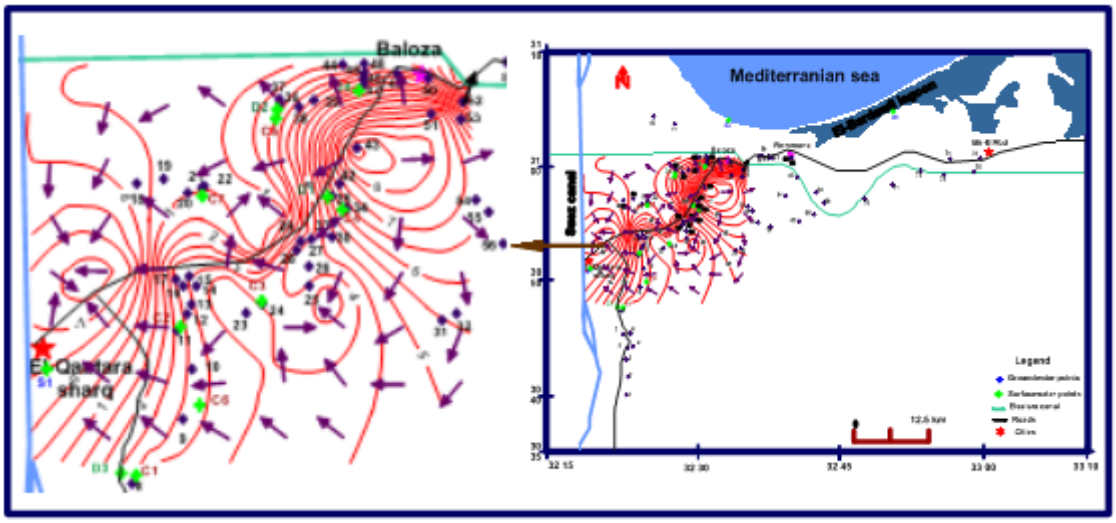

Fig (4): Groundwater flow directions in the quaternary aquifer [7].

3- Sampling and analysis methods:

The water samples were collected from 33 water points during November (2015), 28 samples from groundwater wells and 5 samples from surface water (Suez Canal, Meditranian sea, El-Bardawil lagoon, drain and El-Salam Canal) (Figure. 5).

Temperature, pH value and electrical conductivity (EC) of each sample were measured in situ using portable pH/EC meter (HANNA HI8424 and GLF-100RW conductivity meter). Carbonates and bicarbonates were determined volumetrically by conventional titration. The remaining major ions (CO_3, HCO_3, Cl, Ca^{2+}, Mg^{2+}, Na^{+} and K^{+}) were measured by using ion chromatography (Dionex, ICS-1100 Reagent-Free IC System.

Thirteen water samples (8 from groundwater and 5 from surface water) were selected for environmental stable isotopes (O-18 and deuterium) determination. This analysis was performed at the Nuclear Regulatory and radiological Authority of Egypt (NRRA).

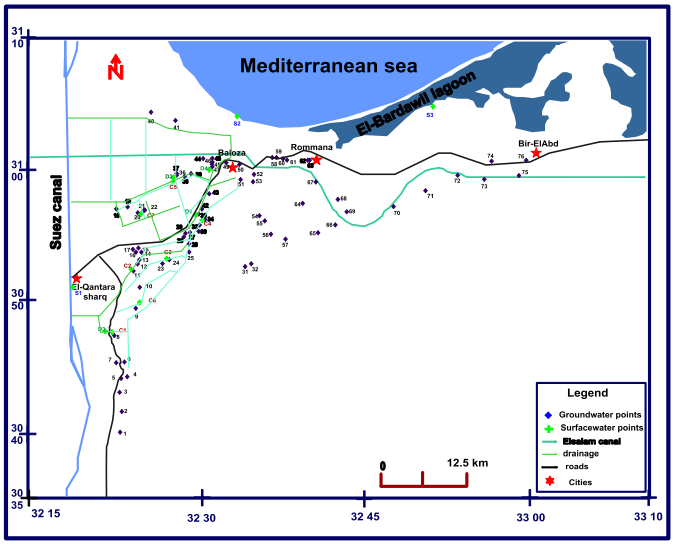

Fig (5): Locations of the water points in the study area.

4- Results and discussion:

4.1 interpretation of physico-chemical parameters:

The results of major ions (anions and cations) of the selected surface and groundwater samples in the study area (Table 1) can be described as follow:

The pH values range from 7.1 to 8.93 indicating an insignificant influence of the anthropogenic contamination that may be resulted from the infiltration of El-Salam canal and its tributaries and agricultural drainage in the study area. This explanation is aided by the results indicated in [8] which concluded that El-Salam canal (The main recharging source to the groundwater) is polluted with coliform bacteria and Sheigella. The presence of such organisms in water affects its pH through their metabolic activities. They called Acidophiles, Neutrophiles or Alkaliphiles if they produce acid, neutral or alkali metabolites, respectively [9]. Bacterial types recorded in El-Salam canal are Neutrophiles and Alkaliphiles which adjusted the pH to a value suitable for their optimum growth conditions. The large variation in the temperature (it ranges from 19°C to 27.7 °C) is attributed to the direct impact of the weather on the shallow unconfined aquifer. The total dissolved solids (TDS) ranged from 275 to 14620 mg/l. This wide range in the salinity is clearly due to the influence of different recharging sources on groundwater salinity. These sources include, rain, El-Salam Canal, drains, Mediterranean Sea and lakes. The TDS contour map (Figure 6) indicates that there is an increase in the groundwater salinity with the flow direction. The sea water influence is clear where the salinity has significantly increased in the samples located in north western part of the study area.

According to [10], about 82 % of the samples are belonged to brackish water type (TDS > 1000 mg/l) and the remaining 18 % are of fresh water type (TDS < 1000 mg/l). Sodium is the most abundant cation in groundwater, it varies from 65 to 4055 mg/l. Calcium is ranging from 9 to 689 mg/l. Magnesium concentration ranges from 11 to 463 mg/l. Potassium ranges from 5.3 to 130.6 mg/l. The chloride in groundwater ranges from 44.6 to 8383.2 mg/l. The sulfate ion ranges from 49.5 to 1601.4 mg/l. The bicarbonate ion ranges from 10.8 to 547.3 mg/l. Nitrate ion in the study area ranges from 9.9 to 190.5 mg/l. The large variation in major ion concentrations can be attributed to same cause that led to the significant change in groundwater salinity in addition to other factors such as, facies change and geochemical processes (ion exchange, leaching and dissolution). These factors can be discussed as follow:

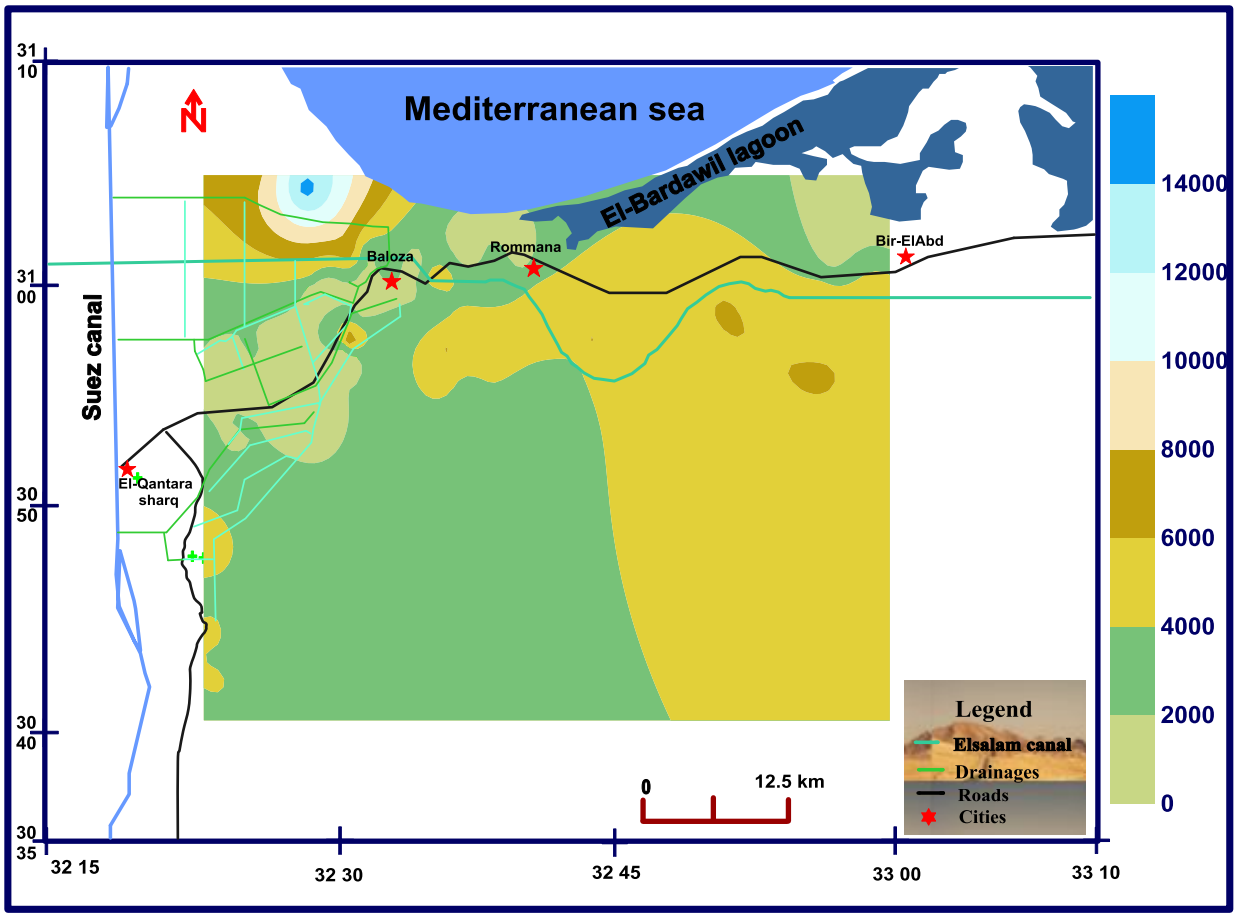

Fig (6): Total dissolved solids distribution map of the investigated groundwater (mg/l)

Table (1): Concentrations of Cations and Anions of water samples in the study area.

No	TDS	Na	K	Mg	Ca	CO_3	HCO_3	Cl	SO_4	alkalinity	T.H
Groundwater											
1	2221	722.0	5.8	23.7	61.6	0.0	142.1	743.2	594.0	118.6	251.2
5	5446	1481.5	9.7	132.7	283.2	0.0	72.2	2001.1	1501.4	59.7	1251.9
9	3229	990.0	68.0	56.9	83.6	6.2	200.2	1122.5	807.6	166.7	442.3
11	1462	465.1	24.8	31.1	36.7	8.2	276.5	564.0	201.6	228.4	219.3
16	1949	431.4	44.6	71.6	145.6	0.0	187.7	759.5	402.6	155.1	657.6
18	1878	577.2	45.7	57.7	30.1	16.4	299.8	702.7	314.7	248.2	311.7
20	969	293.0	33.8	35.8	12.0	16.4	309.8	276.2	163.5	255.9	176.8
23	1378	445.5	12.9	23.3	32.9	8.2	214.3	492.1	263.9	178.4	177.8
25	1366	444.5	13.6	24.1	34.5	10.9	203.2	478.7	268.9	169.4	184.8
27	1414	425.1	16.6	28.7	52.0	2.7	196.5	513.1	280.1	163.9	247.9
31	3471	997.2	10.6	76.2	171.3	0.0	91.1	1587.3	583.1	75.4	740.5
34	1375	385.5	11.2	47.6	60.6	5.5	212.1	547.0	217.3	177.2	346.7
36	2119	412.3	19.0	53.0	221.1	0.0	237.6	387.5	907.6	195.0	770.0
39	1187	287.3	29.7	48.6	69.3	8.2	248.7	386.4	241.6	204.8	372.5
41	14623	4055.4	130.6	689.8	463.4	0.0	385.3	8186.2	905.1	316.9	3986.5
43	1320	385.5	23.5	38.8	47.5	0.0	222.1	497.7	215.4	185.4	278.1
48	1183	326.0	15.4	51.9	48.9	5.5	246.5	415.0	203.1	204.1	334.8
49	4162	1392.4	42.9	81.5	57.8	10.9	209.9	1973.9	508.6	173.8	478.6
50	281	71.2	5.7	12.5	17.7	0.0	171.2	38.6	49.4	142.6	95.6
53	1604	596.8	14.6	20.5	17.6	30.0	547.3	421.9	258.5	452.6	127.9
56	3450	993.8	9.9	69.2	171.6	0.0	70.0	1489.5	680.6	57.9	712.5
58	275	72.1	5.3	12.9	17.2	5.5	171.0	39.8	42.5	152.1	95.9
59	313	80.0	5.6	14.1	21.9	8.2	196.5	43.2	49.5	164.9	112.5
60	2210	641.2	9.4	62.2	89.2	5.5	224.3	903.6	392.3	185.3	477.9
64	4378	1291.2	18.1	98.1	200.8	0.0	101.8	2117.6	601.2	84.1	904.1
65	3400	975.2	15.2	76.4	169.4	0.0	105.5	1508.3	604.3	87.2	736.8
69	5850	1743.5	22.2	137.3	256.1	2.7	121.0	2768.1	863.5	100.0	1203.0
Surface water											
C_5	470	100.5	8.9	20.5	46.2	0.0	197.6	108.8	85.5	164.0	199.7
S_1	34680	10360.7	815.2	1352.3	379.8	10.9	186.5	18021.0	3658.6	153.6	6493.9
S_2	32640	9730.0	820.6	1220.6	333.8	10.9	116.6	17411.8	3063.3	96.3	5838.7
S_3	44330	14027.5	890.1	1409.6	370.5	14.2	105.5	23279.3	4299.3	86.9	6705.8
D_1	2805	846.2	9.4	103.1	59.5	0.0	132.1	1179.7	540.3	109.6	571.4
R	122.5	7.6	3.2	11.3	19.2	0.0	54.3	17.8	36.5	44.6	94.33

All data expressed in mg/l - alkalinity (mg/l as $CaCO_3$) – T.H (total hardness mg/l as $CaCO_3$)
C: El-Salam canal, S1: Suez Canal, S2: Mediterranean Sea, S3: El-Bardawil lagoon, D: Drainage, R: Rain

4-1.1 Major ion chemistry:

4-1.1.1 The hydrochemical coefficients (ion ratios)

Hydrochemical coefficients are necessary to delineate water origin. In addition to identify different processes affecting groundwater quality such as mixing, leaching and ion exchange for establishing chemical similarities among water representing a single geologic terrain or single aquifer [11]. Among these coefficients are the following:

a. rNa^+/rCl^-

Na^+/Cl^- relationship reflects the origin of groundwater, when the value of (rNa^+/rCl^-) is more than unity, it reflects meteoric origin, while the genisis of water will be of marine origin when the value is less than one [12].

In particular, sodium increases linearly with chloride, 22% of the investigated groundwater samples have an rNa^+/rCl^- ratio less than unity due to the leaching and dissolution of marine deposits rich by chloride salts from the water-bearing strata. The values of rNa^+/rCl^- for the majority of groundwater samples (78% of the total samples) are more than unity indicating that, meteoric water recharge.

The scatter plot of Na^+ and Cl^- is strongly linear (The straight line is comfortably fitting through the data) suggesting a mixing trend of more saline water with dilute meteoric water (rain water and El-Salam canal) (Figure 7) [13]. The concurrence of the sodium and chloride values with the mixing line is due to the high solubility product of halite, which is considered the main source of both two elements, 36% of groundwater samples release equal concentrations of Na^+ and Cl^- into the solution indicating that the sources are from halite dissolution [14]. Specific deviations from the sea water equilibrium value, however, could be attributed to water–soil interaction, suggesting additional processes of chloride and sodium enrichment or depletion. Generally, Na^+/Cl^- ratio decreases with salinity increasing indicating that, the groundwater is not evolving towards equilibrium (Figure 8) [15].

Finally, the seawater dilution line in (Figure 7) shows simple mixing of both freshwater (El-Salam canal) and seawater as shown by the Na^+ and Cl^- ion concentration.

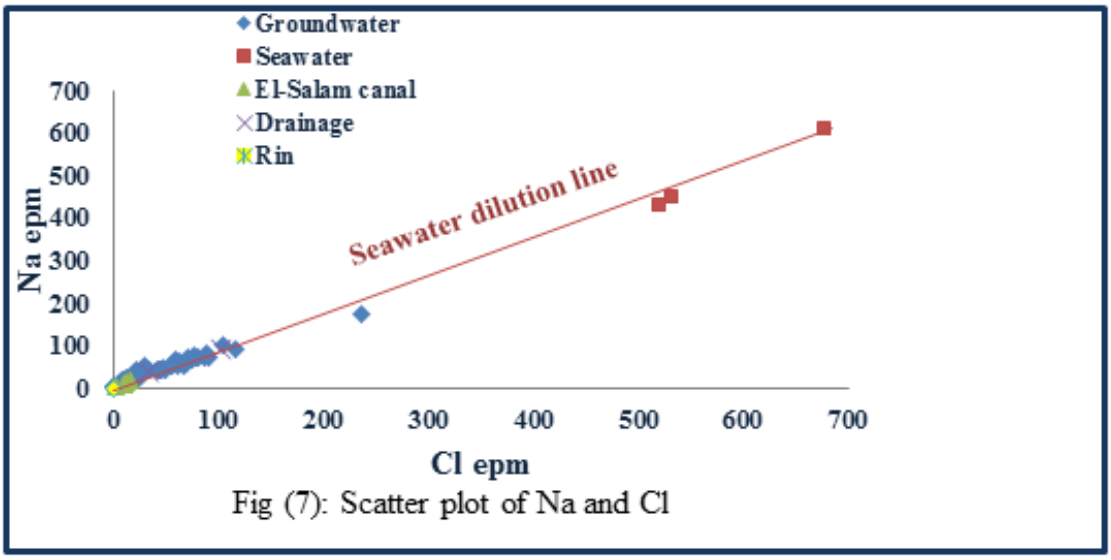

Fig (7): Scatter plot of Na and Cl

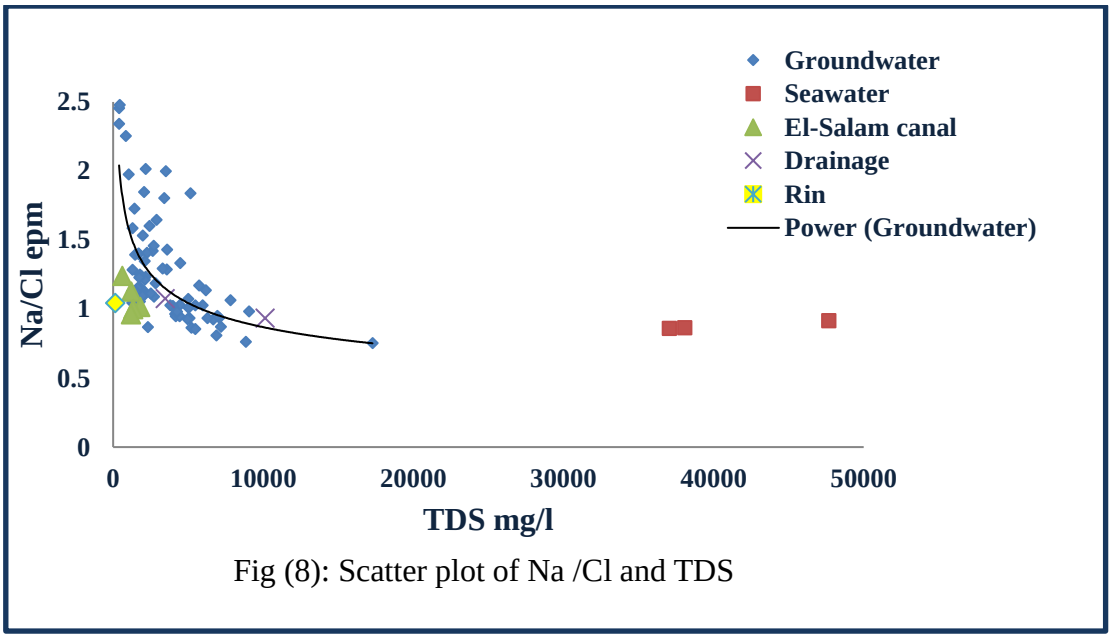

Fig (8): Scatter plot of Na /Cl and TDS

b. rMg^{2+}/ rCa^{2+}

Mg^{2+}/Ca^{2+} ratio of groundwater samples varies from 0.39 to 4.89, the decrease of the ratio with increasing salinity can be attributed to the increase of cation exchange of Ca^{2+} and Mg^{2+} with Na^{+} as salinity increases (Figure 9) [15].

About 53% of groundwater samples have values higher than unity indicating the presence of dolomite and gypsum within aquifer matrix [16]. About 47% of groundwater samples are lower than unity reflecting evaporites dissolution as gypsum and anhydrite or ion exchange.

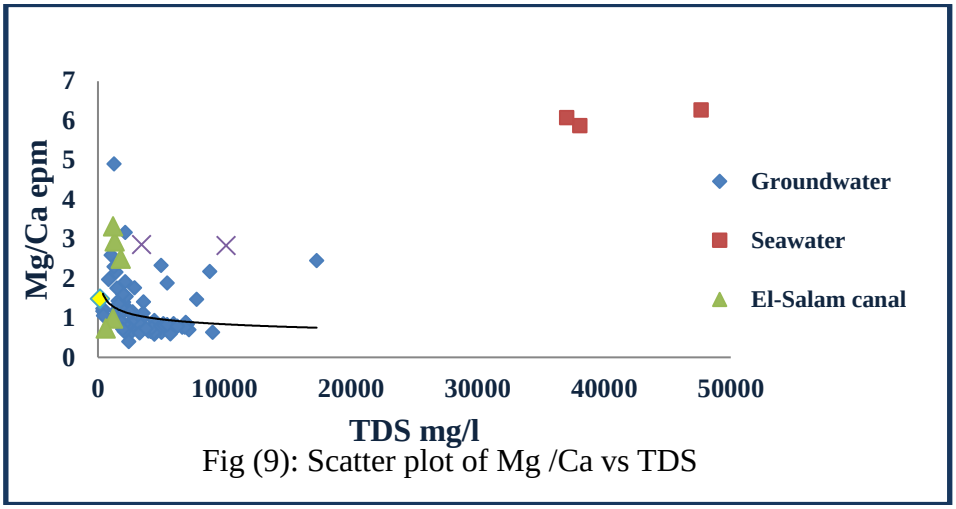

Fig (9): Scatter plot of Mg /Ca vs TDS

c. Cl^{-}/Sum Anions

This ratio gives an indication to the sources of the groundwater [17]. When the ratio is,

> 0.8 and TDS > 500 the source is seawater or brine or evaporites

> 0.8 and TDS < 100 the source is rainwater

< 0.8 the source is rock weathering.

About 87% of the investigated groundwater samples have chloride / sum Anions values less than 0.8 reflecting the impact of rock- weathering Processes. While the rest of groundwater samples reflect the impact of evaporite deposits (Figure 10).

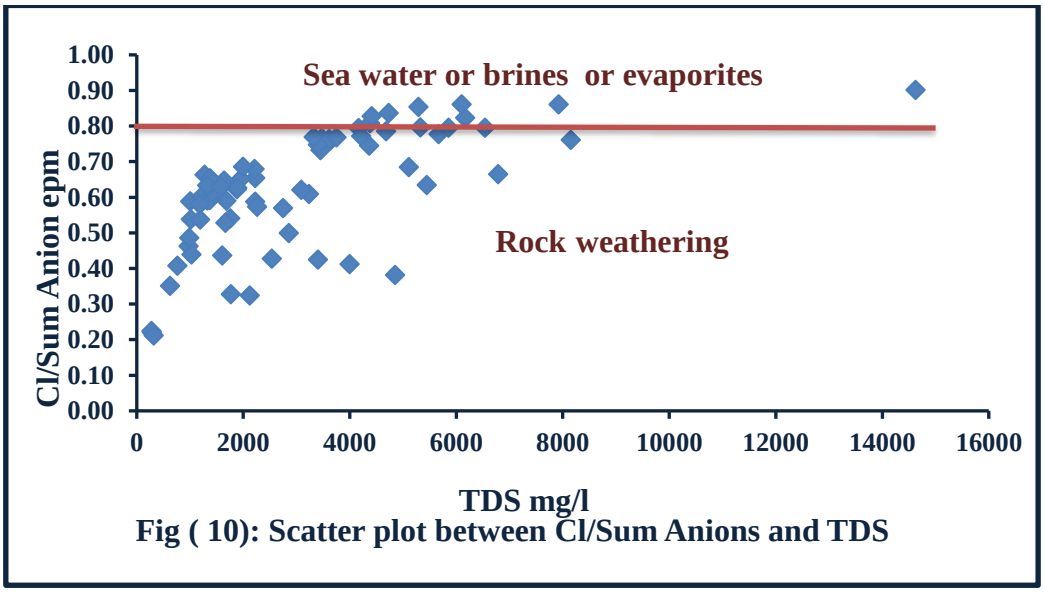

Fig (10): Scatter plot between Cl/Sum Anions and TDS

4-1.1.2-Piper trilinear diagram

According to the plotted chemical data on Piper's diagram (Figure 11), it was shown that all of the groundwater samples are located in the g sub-area except three samples (Nos. 50, 58 & 59) located in Baloza and Rommana localities which are located in f sub-area. This indicates that hydrochemical facies of almost all the groundwater samples belong to alkaline water with prevailing sulfate and chloride while few of them are belonging to alkaline water with prevailing bicarbonate.

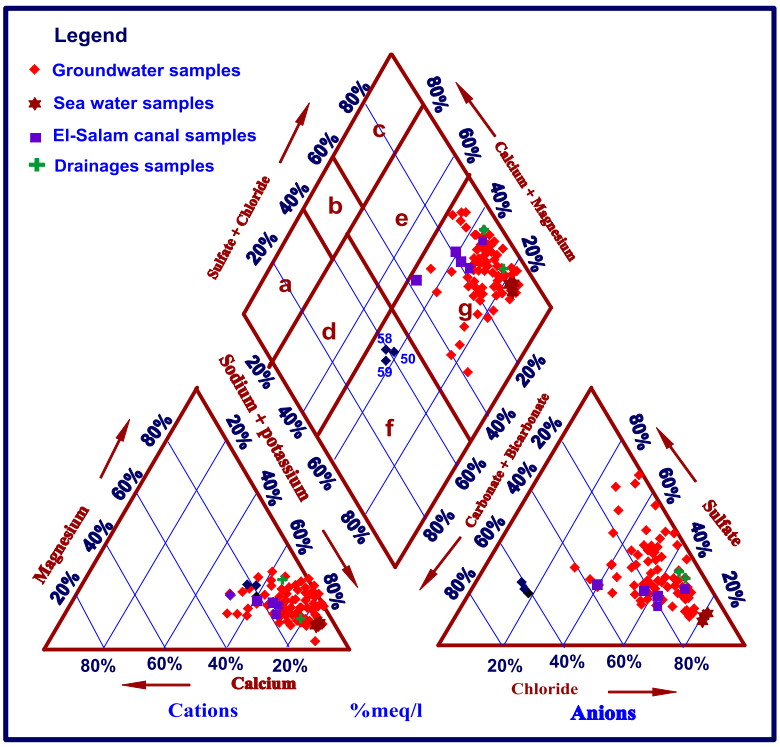

Fig (11): Piper [18] trilinear diagram with langguth [19] classification.

4.2- Geochemical evolution of groundwater:

4.2.1- Geochemical evolution based on Burdon's system [20].

According to [20], the majority of groundwater samples (80%) are belonging to the more advanced grade of metasomatic sequence Cl^{-}> SO_4^{2-} > HCO_3^{-}. This reflects the effect of leaching and dissolution of terrestrial and marine salts through the recharge by rainfall and surface runoff water. On the other hand, 16% of the investigated groundwater is following the less advanced grade of metasomatic sequence SO_4^{2-} > Cl^{-} > HCO_3^{-} and Cl^{-} > HCO_3^{-} > SO_4^{2-}. In addition, three samples only are following the sequence HCO_3^{-} > Cl^{-}> SO_4^{2-} which considered as a transitional stage of evolution (Table 2).

Table (2): Classification of the investigated groundwater in the study area on basis of Burdon's grades of metasomatism [19].

Descent grade	Nos. of water samples	%
HCO_3^{-} > Cl^{-} >SO_4^{2-}	50, 58, & 59.	4
Cl^{-} > HCO_3^{-} > SO_4^{2-}	11, 15 & 20.	8
SO_4^{2-} > Cl^{-} > HCO_3^{-}	6, 19, 21 & 36.	8
Cl^{-} > SO_4^{2-} > HCO_3^{-}	1, 5, 9, 10, 16, 18, 22, 23, 25, 27, 31, 34, 39, 41, 43, 48, 49, 56, 60, 64, 65& 69.	80

4.2.2- Stability relation between water and rock

To distinguish different stages of hydrochemical evolution and identify which geochemical reactions are important in controlling water chemistry, saturation indices must be calculated to evaluate the degree of equilibrium between water and minerals [21]. By using the saturation index approach, it is possible to predict the reactive mineralogy of the subsurface from groundwater data without collecting the samples of the solid phase and analyzing the mineralogy [22].

The saturation indices were determined using the hydrogeochemical equilibrium model, WATEQ4F for Windows.

The saturation index (SI) of a given mineral is defined as:

$$SI = \log_{10} (IAP/KSP)$$ [23].

IAP represents ion activity product and Ksp is the solubility product at a given temperature.

Supersaturating (SI > 0) indicates that precipitation is thermodynamically favorable in spite of the fact that slow rates of reaction can inhibit precipitation. Unsaturation (SI < 0) signifies that dissolution is favored.

The SI for Halite, Calcite, Gypsum, and Dolomite are tabulated (Table, 3) (Figure 12).

Nearly all of the water samples were oversaturated with respect to calcite and dolomite (carbonate minerals) and under saturated with respect to gypsum and halite.

Table (3): Saturation indices values of the surface and groundwater samples in the study

No	Halite	Calcite	Gypsum	Dolomite	No	Halite	Calcite	Gypsum	Dolomite
1	-2.96	0.37	-1.22	0.60	43	-3.44	0.61	-1.61	1.47
5	-2.22	0.33	-0.46	0.63	48	-3.54	0.42	-1.64	1.20
9	-2.64	0.57	-1.09	1.28	49	-2.28	0.26	-1.44	1.01
11	-3.27	0.21	-1.79	0.67	53	-3.27	0.22	-2.00	0.84
16	-3.19	0.58	-1.05	1.18	56	-2.53	0.25	-0.87	0.44
18	-3.10	0.23	-1.77	1.05	60	-2.94	0.46	-1.26	1.10
20	-3.79	-0.17	-2.24	0.46	64	-2.71	-0.62	-0.88	-1.21
23	-3.36	0.35	-1.70	0.87	65	-2.70	0.36	-0.92	0.70
25	-3.37	0.36	-1.67	0.94	69	-2.91	0.50	-0.72	1.07
27	-3.33	0.55	-1.48	1.16			Surface water		
31	-2.51	0.36	-0.93	0.69	S_1	-2.63	0.47	-1.84	0.88
34	-3.37	0.70	-1.55	1.63	S_2	-2.79	-0.17	-0.73	0.52
36	-3.49	0.02	-0.58	-0.27	S_3	-1.78	0.04	-0.76	0.90
39	-3.64	0.23	-1.41	0.63	C_5	-1.78	0.06	-0.47	0.93
41	-1.18	0.94	-0.61	2.06	D_1	-1.78	0.42	-1.09	0.91

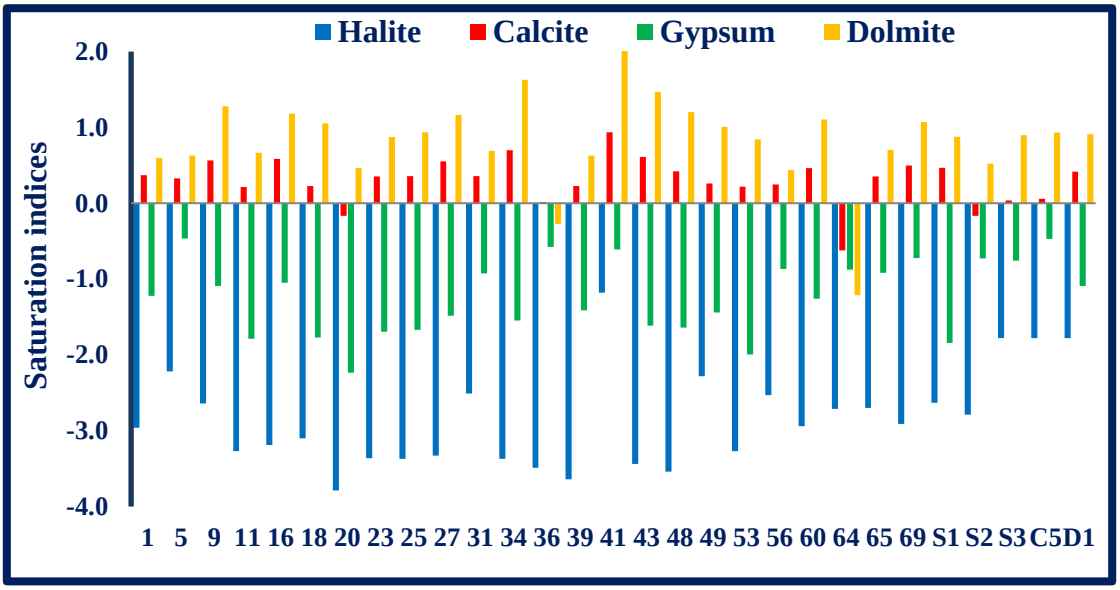

Fig (12): Saturation indices of water samples in the study area

5- Environmental stable isotopes of water

The isotopic compositions of a sample are reported relative to the Vienna Standard Mean Ocean Water (SMOW) reference for both hydrogen and oxygen, and expressed in the delta per mil (δ (‰)) notation:

$$\delta_{sample}\ (‰) = [(R_{sample}/ R_{reference}) - 1]\times 1000$$

Where, δ (‰) is the isotope ratio in delta units relative to a standard, R sample and R standard denote the $^{2}H/^{1}H$ or $^{18}O/^{16}O$ isotopic ratios in the sample and the reference material, respectively [24].

The d-excess (or d parameter or d) is defined as d= δ D - 8 δ ^{18}O. It expresses the non-equilibrium isotopic fractionation between water and vapour during the primary evaporation occurring above oceans and seas water surfaces, d parameter value depends on the climatic conditions (relative humidity, temperature and wind

speed) in the sources of air masses causing the precipitations. It can be used for comparison in groundwater investigations, where it is an indicator of evaporation rates and altitudes where the recharge took place [25].

5.1- The relationship between δ ^{18}O and δ D in groundwater samples

The relationship between ^{2}H and ^{18}O in fresh waters correlates well on a global scale. This relationship is described as the, Global (GMWL) and Mediterranean meteoric water line (MMWL), expressed by the equations:

$\delta\ ^{2}H = 8\ \delta^{18}O + 10$ (GMWL) [26]

$\delta\ ^{2}H = 8\ \delta^{18}O + 22$ (MMWL) [27].

The differences in the vapour pressure of $H_2{}^{18}O$ and ^{2}HOH imports disproportional enrichments in the water phase during evaporation. The difference account for ^{2}H enrichments in water which is roughly 8 times greater than for ^{18}O under equilibrium conditions [24].

Isotopic composition and location of surface, ground, and rainwater for 14 samples were tabulated (Table 4), (Figure 13).

Table (4): Stable isotopes results of water samples in the study area.

N	δ^{18}O%	δD%	d-excess	No	δ^{18}O%	δD%	d-excess
Groundwater samples				Surface water samples			
5	-0.81	-9.02	-2.57	C_1	3.87	25.89	-5.07
2	4.24	27.64	-6.28	D_1	2.91	19.03	-4.25
2	4.65	28.84	-8.36	S_1	1.72	10.37	-3.39
3	-1.77	-16.3	-2.14	S_2	1.90	9.87	-5.33
3	4.77	29.61	-8.55	S_3	5.18	31.08	-10.36
4	4.06	24.66	-7.82	R	-1.42	-9.17	2.19
5	4.75	30.38	-7.62	R: Local rain water (Ismail, et al., 2012)			
5	-1.90	-17.19	-1.99				

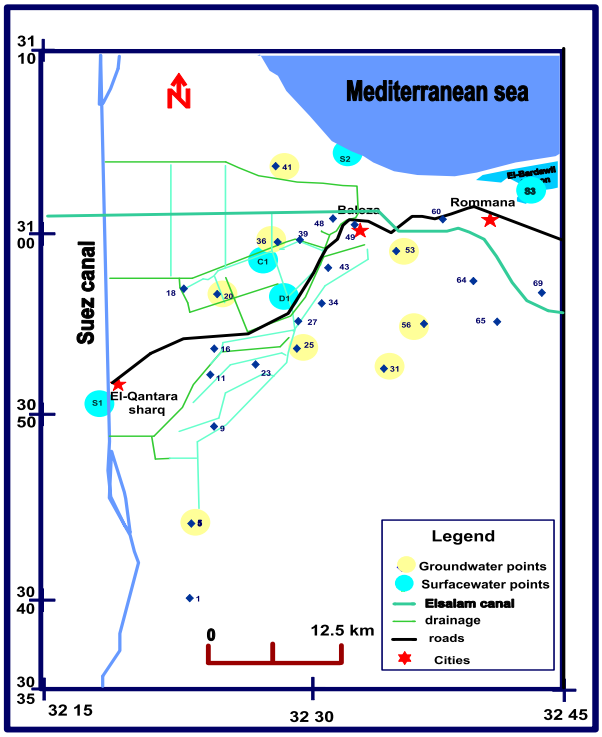

Fig (13): Stable isotopes samples location map.

The isotopic contents of groundwater samples vary in the range from -1.90 % to 4.77 % for ^{18}O and from -17.2 % to 30.38 % for D. While in surface water samples range from 1.72 % to 5.18 % for ^{18}O (avg = 3.12 %) and from 9.87 % to 31.08 % for D (avg = 19.25 %).

This variation may indicate different origins of groundwater and mechanisms of recharge. On a plot of Oxygen-18 versus deuterium (Figure 14), groundwater samples can be classified into two groups.

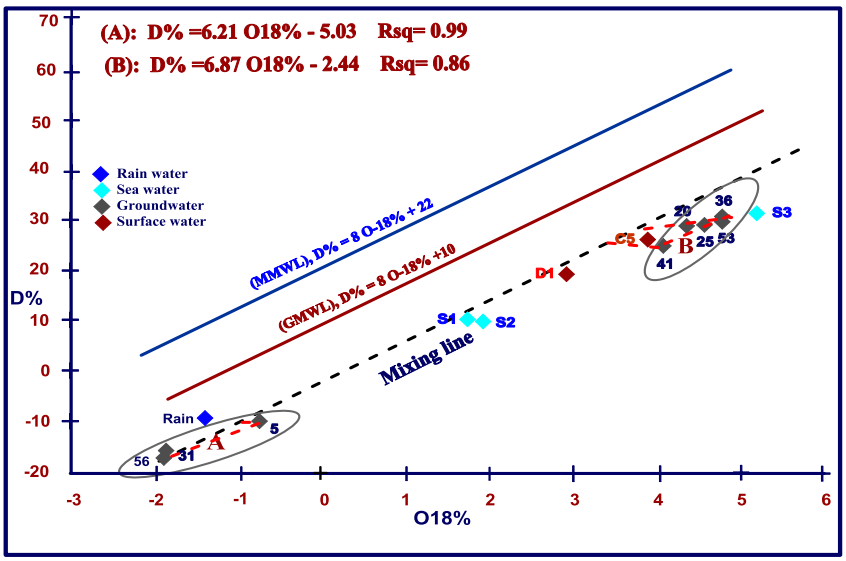

Fig (14): Relationship between D% and O-18% for surface and groundwater samples collected from the study area Global (GMWL) and Mediterranean (MMWL) Meteoric water lines are also shown.

Group A (Samples Nos. 5, 31 & 56) that confirms the contribution from rain water with a high correlation coefficient between ^{18}O and D (R^2=0.99) and trend D = 6.21 ^{18}O% - 5.03. The high correlation coefficient reflects more symmetry and less deviation from equilibrium composition.

Group B (Samples Nos. 20, 25, 36, 41, and 53) with a correlation coefficient (R^2 = 0.86) and trend D = 6.87 ^{18}O% - 2.4, reflecting more symmetry and less deviation from equilibrium. The correlation coefficient of this group is relatively, not high compared with group A. This small difference may indicate the presence of more than one recharging source and different stages according to the influence of mixing of groundwater with surface water (El-Salam canal and its tributaries).

The slight deviation of groundwater samples from meteoric water lines (MWLs) suggests a little evaporation has been occurred. The evaporation had a small impact on the groundwater salinity in the study area. This change is more likely due either the infiltration of the surface waters which have been affected by evaporation or the leaching of salts previously formed by evaporation.

The effect of evaporation on the isotopic composition of groundwater is confirmed by plotting the d-excess values (d-excess = $\delta D - 8\ \delta^{18}O$) against the $\delta^{18}O$ values [28] and [25] (Figure 15).

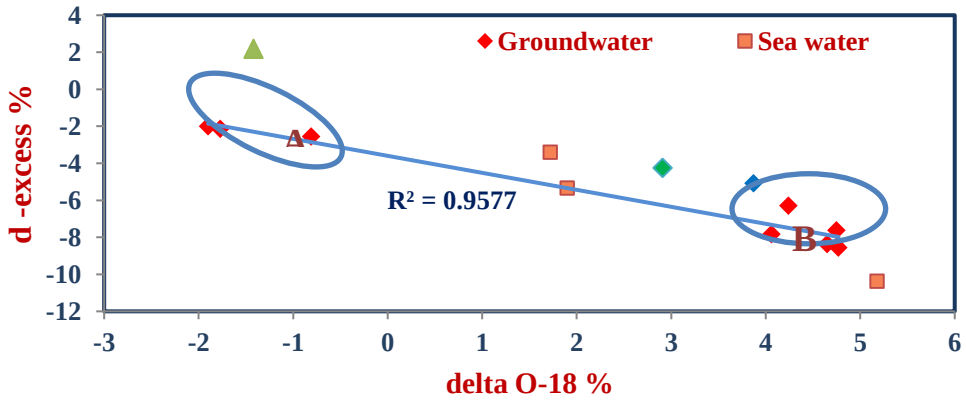

Fig (15): Relationship between d-excess and δ O-18 values of water samples in the study area.

The isotopic parameters are highly correlated (the correlation coefficient, R^2 = 0.957) showing an evaporation trend. The groundwater samples of group B were highly affected by evaporation than group A, where it exhibits low d-excess values and high $\delta^{18}O$ content. Mediterranean Sea water sample is the only lies in the evaporation trend may be indicated the mixing between the groundwater and sea water (sea water intrusion of Mediterranean Sea).

5.2- Sources of salinity in groundwater

Sea water or surface brines are the main source of salinity in the coastal shallow groundwater aquifer. The isotopic data is much better conserved in the aquifer environment than the salinity components, which may undergo processes of ion exchange, precipitation, etc.

Dissolution and flushing of dry salts by precipitation or by other meteoric waters will not result in any change in the isotopic composition [29].

From the relations between the $\delta^{18}O$ and salinity (Figure 16). The relatively high salinity of group A (Nos. 5, 31 & 56) may be due to leaching process during runoff or dissolution process inside the aquifer.

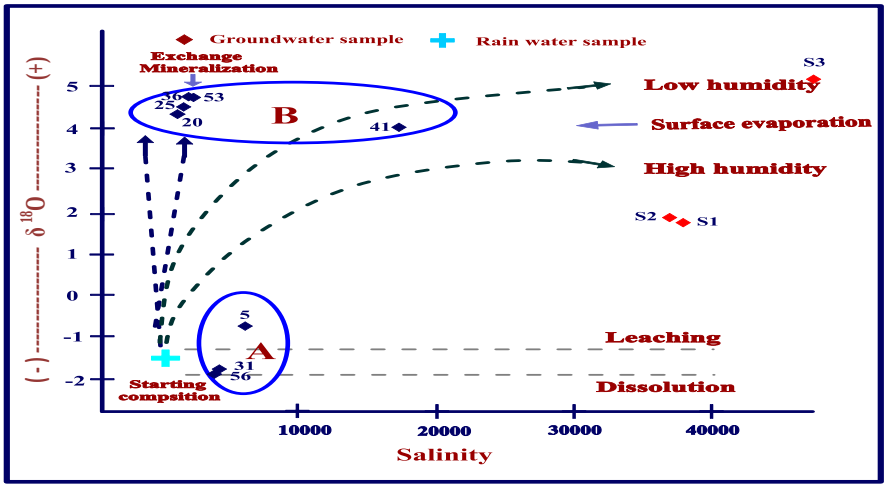

Fig (16): Change in isotopic composition of water, associated with different **salinization processes** [29]

On the other hand, the increase of salinity of group B (nos. 20, 25, 36, 53 & 41) could be attributed to mineralization exchange with slightly influence of evaporation.

5.3- Water rock reaction modeling

Determinations of water–rock interactions, which produce the observed water chemistry and the mineral phases of the aquifers, were identified. This depends on the potential of groundwater flow paths, ^{18}O ‰ data (see Table 4), major-ion chemistry and the relation between isotopic data and major ion concentrations ($\delta^{18}O$ and Cl). Inference of mixing operations utilizing chloride because it is assumed to be a conservative tracer and it is not usually removed from the system due to its high solubility [30], (Figure 17).

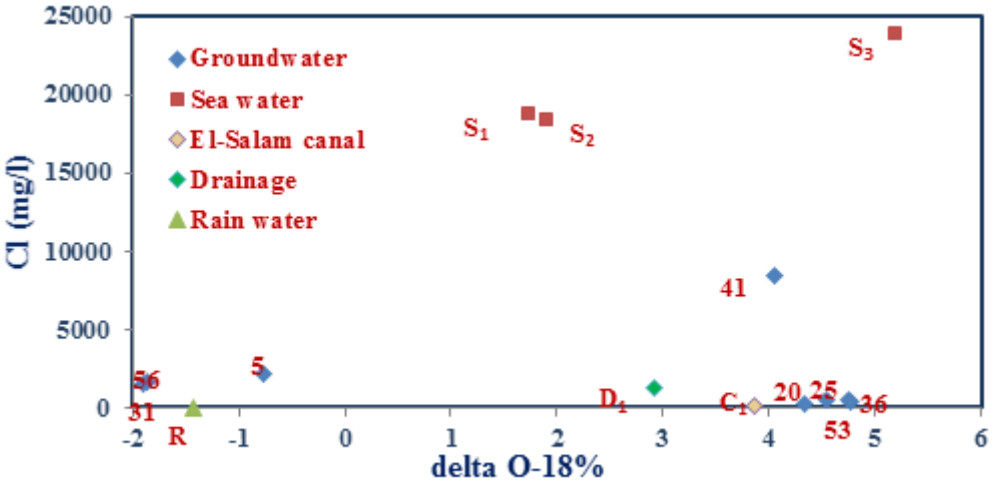

Fig (17): Relationship between Cl and delta O-18 values

Water–rock reaction models developed for this study were constrained by the major-ion concentrations (Calcium, Magnesium, Potassium, Sodium, Chloride, Sulfur and carbon) of the surface and groundwater of the study area. Halite, Calcite, Montmorillonite, Cation exchange, Gypsum, Biotite, Dolomite and Alunite minerals were included as phases in NETPATH models due to the aeolian deposits (sand dune and sand sheets) and alluvial plain deposits (sand mixed with silt and dark clay) that cover most parts of the study area [2].

The changes that may occur in the quality of groundwater as a result of the different geochemical processes or mixing with the different surface water sources were modeled. Potential sources of groundwater were identified by the calculation of the amounts of minerals (in mmol/Kg water) that dissolved or precipitated along the flow path and/or mixing with different sources. For water–rock reaction-model simulation to be considered valid, precipitation or dissolution of any phase

along the proposed flow path could not be greater than 15 mill moles per liter (mmol/l) [31].

The samples used in the model were chosen according to their location along the flow path and their proximity or distance from the recharging sources (Figure 18). The isotopic results obtained in this study are listed in Table 5. The mineralogical evolution of sample no. 20 to sample no. 25 takes place on account of both El-Salam canal water mixing and chemical dissolution / precipitation of salts in the rock/water contact.

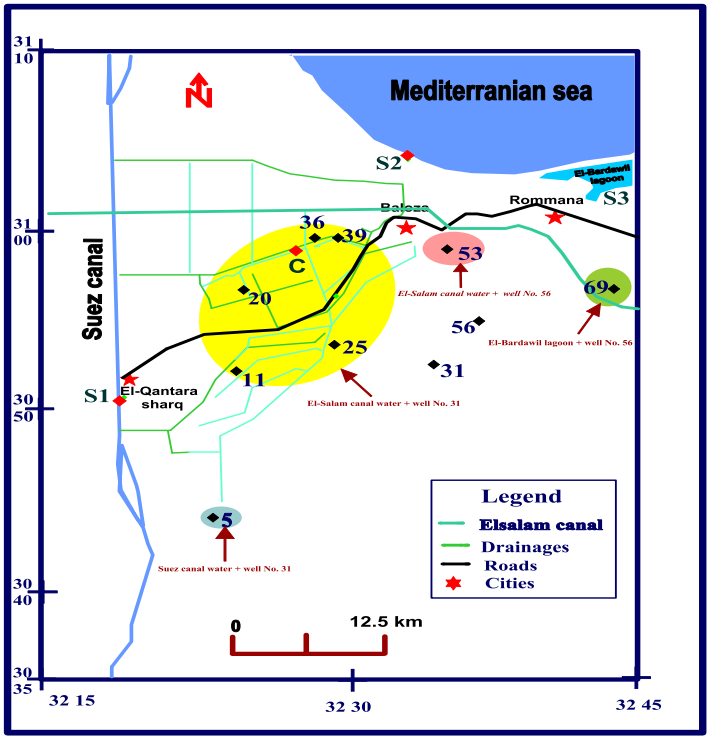

Fig (18): Surface & groundwater mixing zonation map.

Table (5): NETPATH modeling results for water–rock interactions and mass transfer (mmol/l) for the Northwestern portion Sinai.

Model type	Initial (1)	Initial (2)	Final	Mixing (percent)		
				Initial (1)	Initial (2)	
Mixing (A)	C	31	25	75.37	24.63	Based on Cl
			36	81.40	18.60	Based on Cl
			11	69.00	31.00	Based on Cl
			39	80.85	19.15	Based on Cl
	S_1		5	2.77	97.24	Based on Cl
				27	73	Based on ^{18}O
Mixing (B)	C	56	53	76.10	23.90	Based on Cl
	S_3		69	5.98	94.02	Based on Cl
Mixing (C)	C	25	20	54.8	45.2	Based on Cl
				52	48	Based on ^{18}O

Note: Initial waters (25, 31, 56, 25, El-Salam canal (C), El-Bardawill lagoon (S_3) and Suez Canal (S_1)) represent different water sources used as starting water for the inverse NETPATH model.

The mixing ratio is calculated based on O-18 as well as Cl. There is a great deal of match between the mixing ratios calculated in the two cases. This confirms the validity and verifies the model calculations. The

composition of sample no. 20 modified from sample no. 25 as a result of:

1- Mixing of El-Salam canal (C5) with sample no. 25 in the ratio of 54.8% to 45.2%, respectively (based on Cl) or 52% to 48% based on O-18.

2- Further chemical dissolution of halite & calcite and precipitation of dolomite & gypsum.

The mineralogical evolution of sample no. 31 to sample no. 5 takes place on account of both Suez Canal water (S1) mixing and chemical dissolution / precipitation of salts in the rock/water contact. The mixing ratio is calculated based on O-18 as well as Cl. The composition of sample no. 5 modified from sample no. 31 as a result of:

1- Mixing of Suez Canal (S1) with sample no. 31 in the ratio of 97.24% to 2.77%, respectively (based on Cl) or 73% to 27% based on O-18. This difference between the mixing ratios calculated in the two cases may be attributed to presence of sabkhas in well No. 5 location.

2- Further chemical dissolution of halite & gypsum and precipitation of calcite & dolomite.

Generally, NETPATH model suggests that groundwater (exploited from the quaternary aquifer) surrounding El-Salam canal is a mixture of water originated from quaternary groundwater (well No. 31) and El-Salam canal (C) with an average ratio of (76% from El-Salam canal and 24% from groundwater) (Table 5) (Figure, 16).

The influence of sea water (sea water intrusion), on groundwater clearly appears on the effect of Suez Canal (S_1) on well No. 5, and the effect of El-Brdawill lagoon (S_3) on well No. 69 in a ratio of 2.8% & 5.9%, respectively. The mixing ratio is calculated based on Cl ion concentration.

6. Conclusion

Based on different classification of groundwater, the majority of groundwater is alkaline water with prevailing sulfate and chloride. The results showed that, 62% of the groundwater samples are belonging to meteoric origin with the Na-SO_4 type, while about 16% are of meteoric origin with the Na-HCO_3 type. On the other hand, the rest of the groundwater samples are originated from a marine environment (18% represents recent marine origin with the Mg-Cl type and about 4% representing old marine origin with the Ca-Cl type.

The majority of groundwater samples (80%) are belonging to the more advanced grade of metasomatic sequence $Cl^- > SO_4^{2-} > HCO_3^-$. This reflects the effect of leaching and dissolution of terrestrial and marine salts by the rainfall and surface runoff water. On the other hand, 16 % of the investigated groundwater samples are following the less advanced grade of metasomatic sequence $SO_4^{2-} > Cl^- > HCO_3^-$ and $Cl^- > HCO_3^- > SO_4^{2-}$.

According to the values of saturation indices calculated by WATEQ program, nearly all of the water samples are oversaturated with respect to calcite and dolomite and undersaturated with respect to gypsum and halite. This indicates that groundwaters are most likely to precipitate calcite and dolomite and dissolve halite and gypsum minerals.

Environmental stable isotopic relations indicated that the source of groundwater recharge is mainly rain water that originated from the air masses coming from the Indian Ocean. The wide variation of stable isotopes may indicate different origins of groundwater and mechanisms of recharge. The mineralization was developed under the effect of leaching process during runoff or dissolution process inside the aquifer and mineralization exchange with slightly influence of evaporation.

In summary, NETPATH models suggest that the most likely sources of groundwater recharge should include: El-Salam canal water, rain water, El-Bardaweel Lake and sea water. The main recharging source to the groundwater is El-Salam canal with a minor contribution from El-Bardaweel Lake and Suez Canal. The model also indicates that rain water is subjected to alteration in its chemical composition before it leaked to the reservoir. This chemical change is probably due to the dissolution of the salt marches and sand dune sabkhas spread out in some localities in the study area and also due to the evaporation process that affects rain water chemistry before it seeps to the groundwater aquifer.

Recommendations

In order to develop the groundwater in the northwestern portion of Sinai Peninsula the following bases should be taken into account:

1- Routine checks of the quality of the groundwater supply and establishment of environmental monitoring stations in the study area are necessary to ascertain its pollution status.

2- To avoid the effect of the sea water intrusion and to protect the wells against overexploitation (over-pumping), sustainable management and policy actions must be taken by controlling the random drilling of wells by farmers and sharing the use of wells located in one place.

3- The Government should be adopted some treatment technologies to minimize the heavy metals in drainages before mixing with River Nile water in El-Salam canal.

4- It is recommended to control and restrict the agricultural activities in the study area to prevent the leachate from reaching the groundwater.

References

[1] Desert Research Center (D.R.C), "Sustainable agricultural development studies of El-Salam canal project". Final report, DRC, Cairo (in Arabic) (2009).

[2] A. El Sheikh, "Groundwater regime along El-Salam Canal in Baloza-Qatya area, North Sinai, Egypt". Egyptian J. of Desert Res. 58 (2), (2008).

[3] G. Abdallah, "Management of groundwater aquifers along the Mediterranean Sea in Sinai Peninsula". The 2nd. Int. Conf. on Water Resources & Arid Enviro. (2006)
[4] F. Monteiro, S. Sultan, P. Represasl and A. El Sorady, "Joint inversion of gravity and geoelectrical data for groundwater and structural investigation: application to the northwestern part of Sinai, Egypt". Geophys. J. Int. 165 (2006).
[5] H. Elkhedr, R. Shereef, A. El Galladi and B. Pederson, "Geoelectric study on quaternary groundwater aquifers in northwestern Sinai, Egypt". Egyptian Geophysical Society (Egs). J. 2(1), (2004) 69.
[6] A. Yousef & A. El Shenawy, "Environmental monitoring of North Sinai with emphasis on factors affecting the salinity of some sediments". I.C.E.H.M.2000. Cairo Univ. Egypt, (2000) pp. 91-101.
[7] A. El Sheikh, M. El Osta and M. El Sabri, "Study of the phenomenon of groundwater levels rise in south El Qantara Shark area, Ismailia, Egypt". Hydrogeo & Hydrologic Eng. J. 2, (2) (2013) .
[8] E. Hamouda, "Groundwater chemistry and its evolution in the northwestern portion of Sinai, Egypt." Ph.D thesis, Zagazig Univ. Fac. Of Sci., (2015) 156 p.
[9] MT. Madigan, JM. Martinko and J. Parker, "Brock's Biology of Microorganisms" Upper Saddle River, NJ: Prentice Hall, 9 th. ed., (2000) 992 p.
[10] R. Freeze, and J. Cherry, "Groundwater". Prentice Hall, Inc, Englewood Cliffs, New Jersey, U.S.A. (1979) 604p
[11] W. Fetter, "Applied hydrogeology". Charles Merrill pub. Co. A. Bell and Howell company, Columbus, Ohio, (1980) 488.
[12] V. Sulin, "Oil water in the system of natural groundwater". Gostopichezdat, Moscow U.S.S.R. (1946) 215 .
[13] J. Bear, A. Cheng, K. Sorek, D. Ouazar and I. Herrera, "Seawater Intrusion in Coastal Aquifers - Concepts, Methods and Practices". Kluwer Academic Publishers, Dordrecht (1999).
[14] Y. Ostovari, S. Zare, H. Harchegani and K. Asgari, "Effects of geological formation on groundwater quality in Lordegan Region, Chahar-mahal- va- Bakhtiyari, Iran". Int. J. Agri. Crop Sci. 5(17), (2013)1983.
[15] E. Glover, T. Akiti and S. Osae, "Major ion chemistry and identification of hydrogeochemical processes of groundwater in the Accra Plains". Elixir Geol. Sci. J. 50, (2012) 10279.
[16] R. Jacobson, and D. Langmuir, "The chemical history of some spring waters in carbonate rocks". Nat. Wat. Well Ass. J. 8(3), (1970) 5.
[17] A. Hounslow, "Water quality data". Analysis and interpretation, Oklahoma State Univ. Oklahoma, U. S. A (1990).
[18] M. Piper, "A graphic procedure in the geochemical interpretation of water analyses". Trans. Amer. Geophys. Union, 25, (1944) 914.
[19] R. Langguth, "Die Grundwasserverhältnisse im Bereich des Velberter Sattels, Rheinisches Schiefergebirge. Der Minister für Ernährung". Landwirtschaft und Forsten, NRW. Düsseldorf, (1966) 127.
[20] J. Burdon, "Metasomatism of groundwater at depth". UNESCO Course on hydrogeology, Desert Inst. Cairo, Egypt (1958).
[21] N. Aghazadeh, A. Mogaddam , "Assessment of groundwater quality and its suitability for drinking and agricultural uses in the Oshnavieh area, Northwest of Iran". J Environ Prot 1, (2010) 30-40.
[22] J. Deutsch, "Groundwater geochemistry: Fundamentals and applications to contamination". Lewis publishers, New York, U.S.A (1997) .
[23] W. Lloyd, and A. Heathcote, "Natural inorganic hydrochemistry in relation to groundwater, an introduction". Clarendon Press, Oxford (1985).
[24] I. Clark, and P. Fritz, "Environmental isotopes in hydrogeology."Lewis, New York, 5(1997).
[25] S. El- Sayed, H. Sabet and H. Ali, "Appraisal of groundwater in El-Tur area, Southwest Sinai, Egypt". Isotope & rad. Res. J. 43(3), (2011) 605.
[26] H. Craig, "Isotopic variations in meteoric waters". American Association for the Advancement of Science, Sci. J. 133(3465), (1961)1702.
[27] R. Gat, E. Mazor and Y. Tzur, "The stable isotope composition of mineral waters in the Jordan Rift Valley, Israel". Hydrol. J. 76, (1969) 334.
[28] W. Dansgaard, "Stable isotopes in precipitation". Tel/us. 16, (1964) 436.
[29] International Atomic Energy Agency (I.A.E.A), "Stable isotope hydrology: Deuterium and Oxygen-18 in the water cycle". Monograph prepared under the aegis of the I.A.E.A./UNESCO working group on nuclear techniques in hydrology of the international hydrological program, STI. /DOC./10, (1981) 210.
[30] A. Appelo and D. Postma, "Geochemistry, groundwater and pollution". 2nd. edition. Balkama, Rotterdam, (2005) 536.
[31] L. Hershey, M. Heilweil, P. Gardner, B. Lyles, S. Earman, J. Thomas, and W. Lundmark, "Ground-water chemistry interpretations supporting the basin and range regional Carbonate-rock aquifer system (BARCAS) Study, eastern Nevada and western Utah". DHS. Publication No. 41230, Prepared by Desert Res. Inst. Nevada System of Higher Education, Reno, NV. and US. Geological Survey, Reston, VA (2007).